Transactions of the Materials Research Society of Japan 29 [2] 611-614 (2004)

Size Distribution Control of Alpha-iron Nano-particles in Iron-implanted Al_2O_3 by Multi-step Implantation Combined with Moderate Annealing

Shinichiro Mochizuki, Hidehiko Wakabayashi, Tamotsu Toriyama, Isao Sakamoto* and Nobuyuki Hayashi**
Musashi Institute of Technology, Department of Environmental Energy Engineering,
1-28-1, Tamazutsumi, Setagaya-ku, Tokyo 158-8557, Japan
Fax: 81-3-5707-2201, e-mail: hwakabay@sc.musashi-tech.ac.jp
*National Institute of Advanced Industrial Science and Technology
**Kurume Institute of Technology

Size-selective growth of α-Fe particles with diameters of 3-5 nm in α-Al_2O_3 was demonstrated using multi-step implantation of Fe^+ ions into α-Al_2O_3 single crystal combined with annealing at moderate temperatures up to 300 °C. As a result of the size-selective growth of particles, the tunneling magnetoresistive characteristics of such granular system are significantly enhanced.
Key words: implantation, nano-particle, granular materials, tunneling magnetoresistance, CEMS

1. INTRODUCTION

Recently, researches have been done intensively on tunneling magnetoresistance (TMR) effect and its application to high-density magnetic recording heads or non-volatile magnetic random access memories (MRAM) [1]. TMR effect is a phenomenon that electron tunneling probability depends on the orientation of magnetization of two metallic ferromagnets between which a thin insulator is sandwiched: tunneling probability becomes high only when the magnetization of one ferromagnet is in parallel with that of the other. Thus TMR effect has usually been observed in multilayers with a ferromagnetic metal/insulator/ferromagnetic metal structure [2] whose insulator is about one nanometer in thickness. Though observed TMR effects are quite large in such multilayers, extremely precise control of thickness and uniformity are required for insulator layer in fabrication of actual devices.

In the present study, we deal with a granular type TMR material where magnetic tunnel junctions are established between metallic single-domain ferromagnetic nano-particles dispersed in an insulator matrix with nanometer-size inter-particle distances. The magnetization of each particle is fluctuating independently (i.e. superparamagnetic) in a zero applied field so that the electric resistivity of the material is high, whereas it becomes low when the magnetizations of the particles are aligned by applied magnetic fields.

The magnitude of TMR effect for a sample with a zero-field resistance of $R(0)$ and with a resistance of $R(B_a)$ in an applied field of B_a is usually evaluated with the MR-ratio defined by

$$\text{MR Ratio} = \{R(B_a) - R(0)\}/R(0) . \qquad (1)$$

Most granular TMR samples have been prepared by sputtering [3, 4], but we found that an Fe-implanted α-Al_2O_3 with a dose of 1.0×10^{17} ions/cm^2 shows TMR effect with a MR-ratio of about 7% [5], which is nearly twice as large as those observed for sputtered films [6]. Although the value is fairly large for granular materials, a steeper applied field dependence as well as a larger saturation value of the ratio and a lower zero-field resistivity have to be achieved for practical TMR materials. Thus we examined a dose dependence of the MR-ratio in Fe-implanted α-Al_2O_3, and found that the MR-ratio shows a maximum at around a dose of 1.5×10^{17} ions/cm^2 [7]. To correlate this behavior with the aggregation state of the implanted iron atoms/ions, we developed a method to analyze the size distribution of α-Fe particles using conversion electron Mössbauer spectroscopy with applied magnetic fields [8]. As a result of the analysis, it was found that formation of non-spherical "large" particles becomes dominant in samples with doses larger than 1.5×10^{17} ions/cm^2, where "large" means that those particles are no longer superparamagnetic. Therefore, the key issue is how to increase number of superparamagnetic particles (that are mainly formed in samples with low doses) without forming the "large" particles. In this paper, we propose a multi-step implantation combined with annealing at moderate temperatures as a method to control particle size distribution.

2. EXPERIMENTAL

Implantations of 100 keV ^{57}Fe ions into the R-cut plane of single crystal α-Al_2O_3 substrates were performed at room temperature at a beam current density of about 2 μA/cm^2. Implanted Fe atoms are calculated to be distributed around a depth of 50 nm by the TRIM code for the present implantation condition. Annealing was done in a vacuum of about 1×10^{-4} Pa with an infrared image furnace. Resistance measurements were carried out using dc two-probe method at a constant voltage of 40 V in magnetic fields up to 1.4 T applied parallel to the sample surface. Conversion electron Mössbauer spectroscopy with applied magnetic fields (hereafter CEMS) was used to analyze the size distribution of α-Fe fine particles. All the CEMS spectra were measured at room temperature with a He+10%CH_4 mixed-gas-flow

type proportional counter and with a ^{57}Co in Rh source. Magnetic fields up to 0.4 T were applied perpendicular to the sample surface using a NdFeB permanent magnet.

3. RESULTS AND DISCUSSION

3.1 As-implanted sample

CEMS spectrum for an as-implanted sample with a dose of 1.1×10^{17} ions/cm^2 in a zero applied magnetic field is shown in Fig. 1(a). The spectrum can be decomposed into four subspectra, each of which is assigned to superparamagnetic α-Fe fine particles, γ-Fe-like clusters, and two different forms of ferrous (Fe^{2+}) oxides.

When an external field of 0.4 T is applied, the subspectrum for α-Fe particles is modified as shown in Fig. 1 (b), from which the distribution of hyperfine field (B_{hf}) in α-Fe particles can be obtained. The distribution was converted into the particle-size distribution shown in Fig. 3 using a method described in the ref. [8].

3.2 Effect of annealing

Isochronal annealing was performed on a sample with a dose of 1.1×10^{17} ions/cm^2 in four steps at 300, 400, 500 and 600 °C for 1 hour, respectively. Figure 2 shows CEMS spectra measured after each step of the isochronal annealing with an applied field of 0.4 T. The largest change in the CEMS spectrum is observed after the first annealing step at 300 °C. Hyperfine field distributions obtained from each spectrum are also shown in the inset of Fig. 2. The particle-size distributions obtained from the hyperfine field distributions are shown in Fig. 3. The particles with diameters of less than ~2 nm decrease while those with diameters of about 3-5 nm increase as annealing temperature increases. As was pointed out, such a change is almost accomplished at the first step of the isochronal annealing at 300 °C.

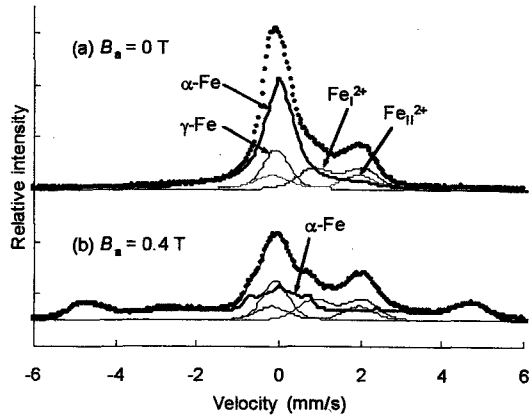

Fig. 1 CEMS spectra (closed circles) decomposed into component subspectra (lines) for an as-implanted sample with a dose of 1.1×10^{17} ions/cm^2; (a) measured in a zero applied field, (b) measured in an applied field of 0.4 T.

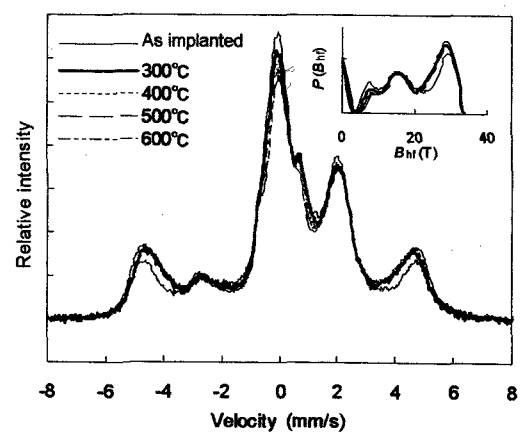

Fig. 2 CEMS spectra for the sample with a dose of 1.1×10^{17} ions/cm^2 measured after each step of the isochronal annealing for 1 hour at 300, 400, 500 and 600 °C with an applied field of 0.4 T. Hyperfine field distributions obtained from each spectrum are shown in the inset.

The zero-field CEMS spectrum measured after the final annealing step at 600 °C is shown in Fig.4. Unlike the spectra measured after the annealing steps at temperatures up to 500 °C, small but definite magnetic splitting is observed in a zero applied field. This indicates that the "large" non-spherical particles with average diameters larger than ~6 nm are formed, and they are no longer superparamagnetic [8].

3.3 Effect of moderate annealing

In order to look in the effect of annealing at temperatures lower than 300°C, isochronal annealing for 1 hour was done on another sample with a dose of 1.1×10^{17} ions/cm^2 at 180, 210, 240 and 270°C, and CEMS measurements were performed after each step of the annealing. The size distributions of α-Fe particles for the sample obtained from these CEMS spectra are shown in Fig. 5. As was seen for the annealing at higher temperatures, number of medium size particles with diameters of about

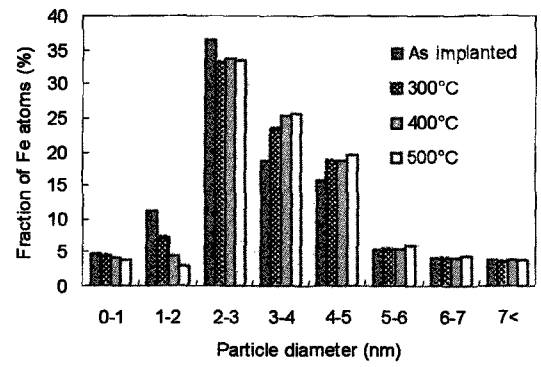

Fig. 3 The α-Fe particle-size distribution in the sample with a dose of 1.1×10^{17} ions/cm^2 obtained after each step of the isochronal annealing for 1 hour. Annealing temperatures for each step is indicated in the legend.

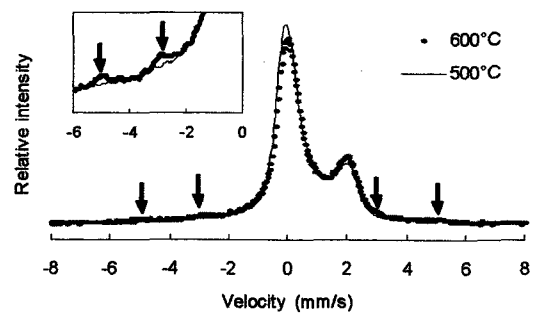

Fig. 4 Zero-field CEMS spectrum for the sample with a dose of 1.1×10^{17} ions/cm^2 measured after the final isochronal annealing step at 600 °C. The spectrum measured after the annealing step at 500 °C is also shown for comparison. The arrows indicate the position of four lines of the magnetically split sextet.

3-5 nm is increased at the expense of particles smaller than ~3 nm without growing particles larger that ~5 nm. It was also confirmed separately that any detectable change is not observed in CEMS spectra after annealing at temperatures below 150°C.

Figure 6(a) shows MR-curves measured after some of the moderate isochronal annealing steps. The MR-curve for the sample isochronally annealed up to 600 °C as well is shown for comparison. The absolute value of MR-ratio at the highest applied field of 1.4 T for each MR-curve is also plotted in Fig. 6(b). For the isochronal annealing step with a higher annealing temperature, the field dependence of the MR-ratio becomes steeper and the absolute value at the highest applied field of 1.4 T increases in the moderate annealing, but the value decreases significantly when the sample is isochronally

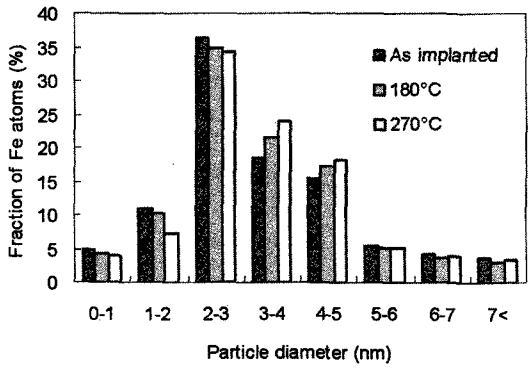

Fig. 5 Size distributions of the α-Fe particles in the sample with a dose of 1.1×10^{17} ions/cm^2 obtained after the moderate isochronal annealing steps at 180 and 270 °C.

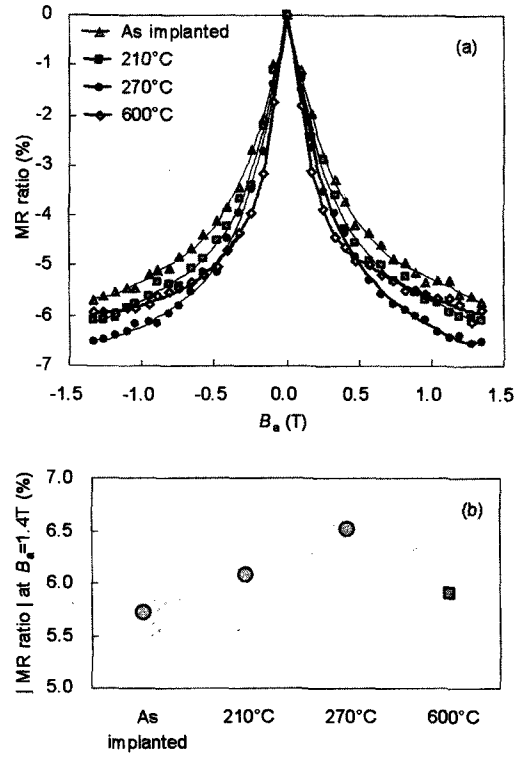

Fig. 6 (a) MR-curves for the sample with a dose of 1.1×10^{17} ions/cm^2 measured after some of the moderate isochronal annealing steps. MR-curve for the sample isochronally annealed up to 600 °C is also shown for comparison. (b) The absolute value of MR-ratio at the highest applied field of 1.4 T for each MR-curve shown above.

annealed up to 600 °C, where non-superparamagnetic "large" particles are formed as was noted previously. The zero-field resistance shown in Fig. 7 also increases with increasing temperature as annealing-step proceeds, but it exhibits drastic increase when the sample is isochronally annealed up to 600 °C.

Since the increase in the zero-field resistance (i.e., the decrease in zero-field tunneling probabilities) implies the increase in inter-particle distances, we may conclude from the change in the particle-size distribution that, with moderate annealing at temperatures below 300 °C, small particles with diameters less than ~3 nm are integrated into medium size particles of 3-5 nm without further evolution of particles larger than ~5 nm.

The mechanism of such a change in microstructure caused by the moderate annealing is not yet understood well. However, the annealing temperature of 300 °C is obviously too low for normal diffusion of Fe atoms to take place. Thus it seems to have something to do with the recovering process of implantation damages introduced in the α-Al_2O_3 matrix. It should be noted that the moderate annealing temperature of 300 °C is quite favorable in actual device production processes.

3.4 Multi-step implantation with moderate annealing

Our goal is to form medium size superparamagnetic particles as many as possible in the implanted surface, avoiding a growth of large particles and an increase in

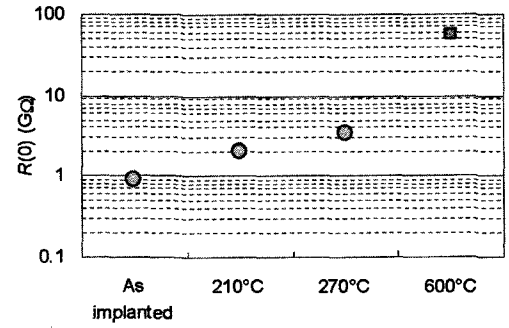

Fig. 7 Zero-field resistance for the sample with a dose of 1.1×10^{17} ions/cm^2 measured after the moderate isochronal annealing steps at 210 and 270 °C. Zero-field resistance for the as implanted sample and the sample isochronally annealed up to 600 °C are included.

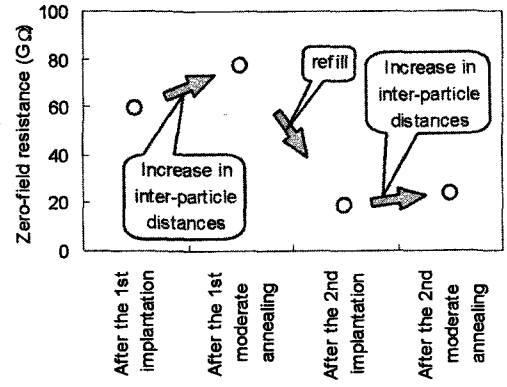

Fig. 8 Change of zero-field resistance measured after each step of the multi-step implantation with moderate annealing which consists of the first implantation with a dose of 0.75×10^{17} ions/cm^2, the first moderate annealing at 300 °C for 2 hours, the second implantation with a dose of 0.35×10^{17} ions/cm^2 and the second moderate annealing at 300 °C for 2 hours.

inter-particle distances, both of which degrade the TMR characteristics. However, a simple high-dose implantation with a conventional annealing leads to the growth of large particles at the expense of small and medium size particles. If the effect of moderate annealing is taken into account, this problem is expected to be solved by a multi-step implantation, in which a low-dose implantation followed by moderate annealing is repeated until certain final dose is achieved. In a low-dose implantation, small particles are dominantly formed. When a moderate post-annealing is carried out, the small particles are integrated into medium size particles, so that unfilled space is enlarged in the matrix. Accordingly, only small particles may be formed again in the subsequent low-dose implantation into such spaces.

Thus we have first prepared a Fe-implanted sample with a relatively low dose of 0.75×10^{17} ions/cm^2, and a moderate post-annealing at 300°C for 2 hours was carried out. Then, a second implantation with a dose of 0.35×10^{17} ions/cm^2 followed by the same moderate post-annealing was carried out. The increase in inter-particle distances by the moderate annealing and the refilling of the enlarged unfilled spaces are well reflected in the changes of zero-field resistances measured after each step of the above multi-step implantation as shown in Fig. 8. It was also confirmed in the particle-size distribution shown in Fig. 9 obtained from CEMS measurements that more fine particles with diameters less than ~2 nm are formed in the multi-step (two-step, in this case) implantation with the moderate annealing than in a single step implantation with the same total dose (see the part highlighted with a dotted circle in Fig. 9). This means that in the second implantation the small particles are dominantly formed in the unfilled space enlarged by the preceding moderate annealing. Increase in medium size particles by the second moderate annealing was also observed.

It is remarkable that the MR characteristics are greatly improved by the adoption of the multi-step implantation as shown in Fig. 10. The absolute value of the MR-ratio at 1.4 T obtained after the second implantation is the largest among those obtained so far, and it is 1.4 times as large as that for a sample prepared by the single step implantation with the same total dose. Moreover, the value is further increased by the second moderate annealing.

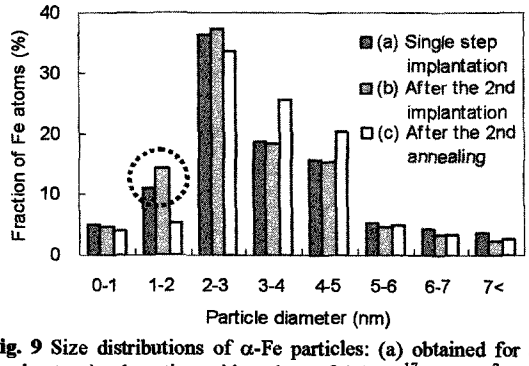

Fig. 9 Size distributions of α-Fe particles: (a) obtained for a single step implantation with a dose of 1.1×10^{17} ions/cm^2, (b) obtained after the second implantation step of multi-step implantation with a dose of 0.35×10^{17} ions/cm^2, (c) obtained after the second annealing step of multi-step implantation at 300 °C for 2 hours. For (b) and (c) the first implantation dose was 0.75×10^{17} ions/cm^2 and the first moderate annealing was done at 300 °C for 2 hours.

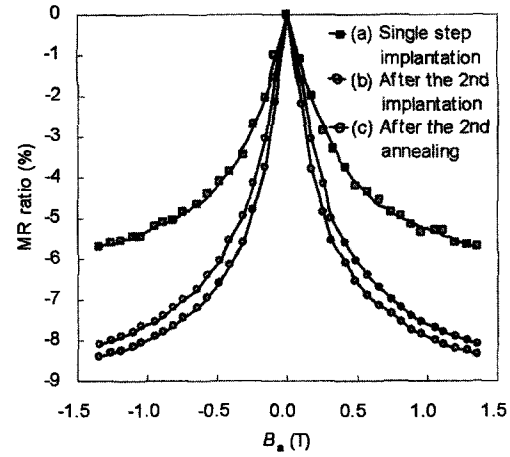

Fig. 10. MR-curves for Fe-implanted α-Al_2O_3 samples prepared by (a) a single step implantation with a dose of 1.1×10^{17} ions/cm^2, (b) and (c) by a multi-step implantation. For (b) and (c), see the caption for Fig. 9.

4. CONCLUSIONS

The following conclusions were reached.

With a moderate annealing at temperatures of 180 -300°C; 1) small particles with diameters less than ~2 nm are integrated into medium size particles with diameters of about 3-5 nm; 2) as a result, inter-particle distances increase and the zero-field resistance of the sample increases; 3) growth of large particles with diameters larger than ~5 nm is not observed.

In the each implantation step of the multi-step implantation that consists of low-dose implantation /moderate annealing sets, formation of particles smaller than ~2 nm are dominant in the unfilled space in a matrix regenerated by the preceding moderate annealing step. Accordingly, combination of multi-step implantation with moderate annealing allows the size-selective growth of the medium size particles without growing non-superparamagnetic (normal ferromagnetic) large particles, and as a results, MR characteristics are significantly enhanced.

REFERENCES

[1] K. Inomata: IEICE Trans. Electron. **E84-C**, 740-746 (2001).
[2] T. Miyazaki and N. Tezuka: J. Magn. Magn. Matter., **139**, L231-L234 (1995).
[3] H. Fujimori, S. Mitani and S. Ohnuma: Mater. Sci. Eng., **B31**, 219-223 (1995).
[4] S. Honda, T. Okada, N. Nawate and M. Tokumoto: Phys. Rev., **B56**, 14566-14573 (1997).
[5] I. Sakamoto, S. Honda, H. Tanoue, N. Hayashi and H. Yamane: Nucl. Instr. Meth., **B148**, 1039-1043 (1999).
[6] S. Mitani, Y. Shintani, S. Ohnuma and H. Fujimori: J. Magn. Soc. Jap., **21**, 465 (1997).
[7] N. Hayashi, I. Sakamoto, H. Tanoue, H. Wakabayashi, and T. Toriyama, Hyperfine Inter. **141/142**, 163-168 (2002).
[8] H. Wakabayashi, T. Hirai, T. Toriyama, N. Hayashi, and I. Sakamoto: phys. Stat. Sol., **(a) 189**, 515-520 (2002).

(Received October 9, 2003; Accepted January 20, 2004)